International Journal of Engineering Innovation & Research
Volume 3, Issue 4, ISSN: 2277 – 5668

Optimum Design of Single-Sided Linear Induction Motors using Particle Swarm Optimization

Sabiyeh Niknafs
MSc Student, Islamic Azad University, Borujerd Branch, Borujerd, Iran
Email: nafs.niknafs11@gmail.com

Abbas Shiri
Electrical Engineering Department, Islamic Azad University, Hadishahr Branch, Hadishahr, Iran
Email: abbas_shiri@iust.ac.ir

Mohammad Reza Alizadeh Pahlavani
Faculty of Electrical Engineering, Malek-Ashtar University of Technology (MUT) Tehran, Iran
Email: Mr_Alizadehp@iust.ac.ir

Abstract **– In this Paper, by using a mathematical model, the analysis of the dynamic response of a linear induction motor as an electromechanical system is done. Employing the presented model, a feedback control system is proposed to analyze the controlled response of the motor. This procedure is done by analytical method and PI controller which the coefficients of the latter are set by using the particle swarm optimization technique. The results show the accuracy of the model and the improvement of the objective functions at the end of the optimization procedure.**

Keywords **– Linear Induction Motor (LIM), Aircraft Launcher, PI Controller, Particle Swarm Optimization.**

I. INTRODUCTION

The history of the Linear Induction Motors (LIM) goes back to 19th century, a few years after the discovery of the Rotary Induction Motors' (RIM) principle. In general, the operation of a RIM is defined by the interaction of two main parts: the stator (or primary) and the rotor (secondary). The stator consists of a cylindrical slotted structure formed by a stack of steel laminations [1]. The relative motion between the rotating magnetic field and the conductors of the rotor induces a voltage in the rotor producing currents flowing through the conductors which also generates its own magnetic field. The interaction of these two magnetic fields will produce an electromagnetic torque that drags the rotor in the same direction of the magnetic fields [2]. From the RIM principle, the operation of the LIM can be explained if one imagines the cylindrical slotted structure and the rotor to cut open and rolled flat causing the magnetic fields to travel in a rectilinear direction instead of rotating. However, contrary to the RIM, the LIM has leading and trailing edges[3]. This specific characteristic of the LIM causes the so-called "end effects" that adversely influences the motor performance and basically causes a field distortion at the entry and exit of the mobile part. Similar to RIM, the equivalent circuit model is widely used to study the performance of LIM. In literature, many authors have modeled the end effect phenomenon. This paper has employed one of them to develop the analysis and response of the system [4]. LIMs have been used in many applications in industry such as [5]: machine tools, material handling and storage, accelerators and launchers, low and medium speed trains, sliding doors operation, and other applications which need rectilinear displacement [6]. Different methods have been presented for analysis of the LIMs, such as equivalent circuit model (ECM), 1-D and 2-D electromagnetic field analysis, and numerical methods including finite-element and finite-difference methods [7]–[10]. The motivation for this paper is to implement a feedback control system considering the applications and conditions similar to aircraft launcher systems. A PI controller is used to regulate the power source of the system in terms of the frequency and voltage amplitude, allowing the LIM to overcome certain disturbing forces or changes in the desired speed reference. The parameters of PI controller are tuned by Particle Swarm Optimization algorithm.

II. PERFORMANCE MODEL APPROACH FOR THE ESTABLISHMENT OF THE EQUIVALENT CIRCUIT

First, a brief description about the "end effect" is done for a better understanding of the system [11]. Then, considering this effect, the equivalent circuit model for a LIM will be presented similar to the rotary induction motor. Figure 1 illustrates the configuration and some important aspects related to the end effects of this machine. This figure, shows the end effect as the primary moves to the left. The motor is feed by 3-phase currents which produce a sinusoidal MMF per unit length and a sinusoidal flux density [12],[13]. As the primary moves, new material (in the secondary) enters in the leading edge of the motor where eddy currents rise to their maximum value, and the flux density reduces to zero, and start growing with a time constant T_2 as the eddy currents fade away. T_2 is defined as follows:

$$T_2=\frac{(L_m+L_{21})}{R_{21}} \quad (1)$$

T_2 is called the total secondary time constant.

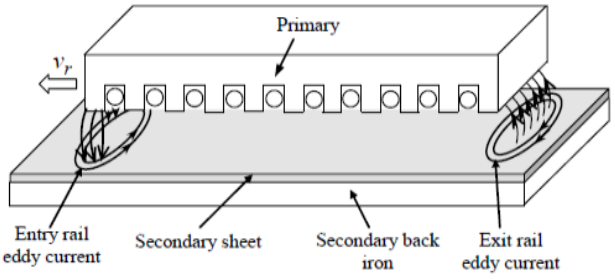

Fig.1. Side view of a Linear Induction Motor (LIM)

The normalized length of the motor is defined as:

$$Q = \frac{DR_{21}}{(L_m+L_{21})v_r} \quad (2)$$

International Journal of Engineering Innovation & Research
Volume 3, Issue 4, ISSN: 2277 – 5668

Now, the next step is to quantify and represent these end effects into the per phase equivalent circuit of the LIM. According to reference [4], these parameters are:

At the entry section of the primary, the demagnetizing effect of eddy currents, represented as an inductor in parallel with L_m:

$$L_m \frac{I_{mea}}{I_{2ea}} = L_m \{\frac{Q}{1-e^{-Q}}\text{-}1\} \quad (3)$$

The following expression is the modified magnetizing inductance:

$$L_m \{1\text{-} \frac{1-e^{-Q}}{Q}\} \quad (4)$$

The current I_m is derived as: $I_m = I_{mea}+I_{2ea}$.

Ohmic losses due to eddy currents for a resistance R_{21} of the circuit:

$$\text{Eddy current losses} = I_m^2 \; R_{21} \frac{1-e^{-2Q}}{2Q} \quad (5)$$

As the motor passes the rail over, the MMF seen by the rail disappears and eddy currents will rise in order to maintain the gap flux, as depict in Figure 2. The magnetic energy is then dissipated in the resistance, and the power loss is defined by the following expression:

$$\text{Exit power loss} = I_m^2 \; R_{21} \frac{\{1-e^{-Q}\}^2}{2Q} \quad (6)$$

And adding equations (5) and (6) the ohmic loss due to eddy currents is defined by:

Total ohmic losses due to eddy currents in rail $= I_m^2 \; R_{21} \frac{\{1-e^{-Q}\}}{Q}$ (7)

These losses are represented in the equivalent circuit as a resistance in the magnetizing branch dependent on the vaue of Q :

$$R_{21} \frac{\{1-e^{-Q}\}}{Q} \quad (8)$$

Thus, considering equations (4) and (8), Figure 2 represents the equivalent circuit of a linear induction motor (LIM):

Where V_1 is the phase voltage of the LIM, R_1 the primary resistance which indicates heating losses in the primary coils, L_1 indicates leakage flux of the primary, L_M represents the magnetizing flux linking the primary and secondary, R_{21} the secondary resistance referred to the primary which indicates heating losses in the secondary, L_{21} indicates leakage flux of the secondary referred to the primary. For sheet secondary single-sided LIM, L_2 is negligible. In DSLIM, the back iron is replaced with another primary; however, all the relations mentioned previously holds. Also, $L_m \{1\text{-}\frac{1-e^{-Q}}{Q}\}$ is non-linear function that represents the resultant magnetizing flux in the air gap. $R_{21} \frac{\{1-e^{-Q}\}}{Q}$ is non-linear function that represents the ohmic loss in the secondary due to eddy currents.

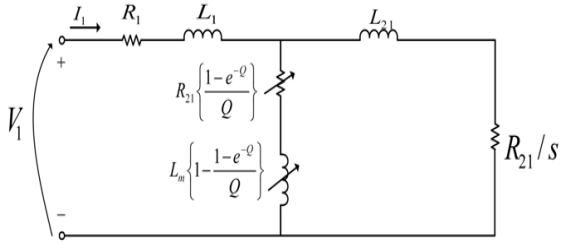

Fig.2. Per phase equivalent circuit of LIM

By using the presented equivalent circuit model we can calculate the normal forces of linear induction motors. The normal forces can be divided into two components. The first component is due to the attraction between the back iron of the primary and the secondary, due to the main flux crossing the air-gap which is defined as:

$$F_{va} = K_a L_m I_M^2 \{1\text{-}\frac{(1-\exp(-Q))(3-\exp(-Q)))}{2Q}\} \quad (9)$$

where K_a is constant. The second component is repulsive force between the secondary current I_{21} and the primary which is defined as:

$$F_{vr} = K_r \frac{I_{21}^2}{d} \quad (10)$$

In the above equation, K_r is constant and d is the distance between the midpoints of the primary and secondary current layers. In double-sided linear induction motors, the effects of the normal forces canceled each other.

On the other hand, Duncan defines the total thrust of the motor as the one generated by the slip currents minus the one due to eddy currents, show as follows:

Motor thrust due to slip currents:

$$3I_{21}^2 R_{21} \frac{\pi}{\omega_2 \tau} \text{N} \quad (11)$$

Motor thrust due to eddy currents:

$$I_M^2 R_{21} \frac{1-\exp(-Q)}{vQ} \text{ N} \quad (12)$$

Where:

τ : motor pole pitch.

ω_2: slip frequency.

III/. Dynamic Analysis and State-Space Equation

In this section, using the equivalent circuit model, a dynamic analysis is done for the LIM. Then, the state-space equation is derived for control analysis.

Recalling the following equation for f(Q) as[14]:

$$f(Q) = \frac{1-e^{-Q}}{Q} \quad (13)$$

we can apply the Kirchhoff's voltage law on the equivalent circuit shown in Figure 2 and get:

$$V_1 = I_1 R_1 + L_1 \frac{dI_1}{dt} + (I_1 - I_{21}) R_{21} f(Q) + \frac{d}{dt}[L_m (1\text{-}f(Q))(I_1 - I_{21})] \quad (14)$$

$$0 = L_2 \frac{dI_{21}}{dt} + I_{21} \frac{dR_{21}}{dt} + (I_{21} - I_1) R_{21} f(Q) + \frac{d}{dt}[L_m (1\text{-}f(Q))(I_{21} - I_1)] \quad (15)$$

$$I_1 = I_{21} + I_m \quad (16)$$

Where s is the motor slip which is defined as:

$$S = \frac{v_s - v_r}{v_s} \quad (17)$$

In the above equation, v_r is the rotor speed and v_s is the synchronous speed which is given as:

$$v_s = 2f\tau \quad (18)$$

IV. Dynamic Simulation of the LIM

Simulation of the LIM as an electromechanical system is performed using the MATLAB/Simulink. The mechanical equation of the system can be written as follows:

$$m\ddot{x} + b\dot{x} + kx = W_{em} - W_d(t) \quad (19)$$

where m is the rotor and load mass, b is the damping coefficient and k is elastic coefficient. Also, W_{em} is the electromagnetic thrust of the LIM and W_d is a disturbance force. the electrical and mechanical parameters are given in appendix A. the simulink model of the system is illustrated in figure 3.

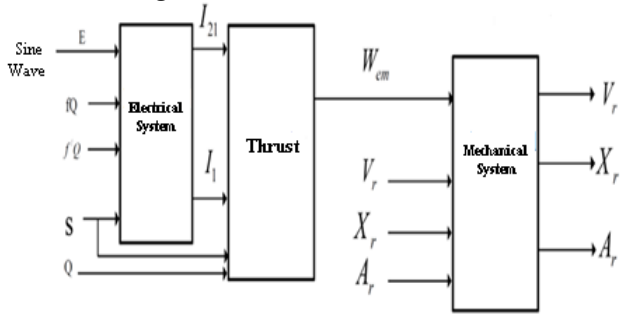

Fig.3. Simulink model of the studied system

Figure 4, shows the stator and the rotor currents versus time. It is seen that at starting, when the rotor speed is zero, the peak initial values of the currents for both of the stator and rotor are almost 400 A. After the rotor starts moving, the stator current decays to less than half of the starting value. It is clear that the rotor speed reaches to zero in steady-state. Figure 5 shows the acceleration and the speed of the rotor versus time. The maximum value of the acceleration occurs at starting which is about 14 m/s^2.

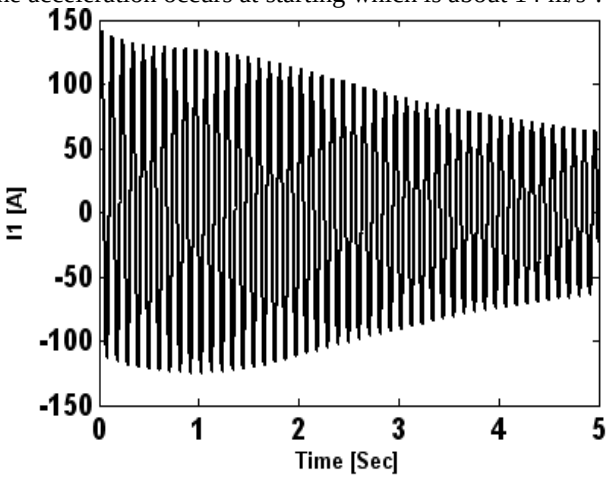

(a)

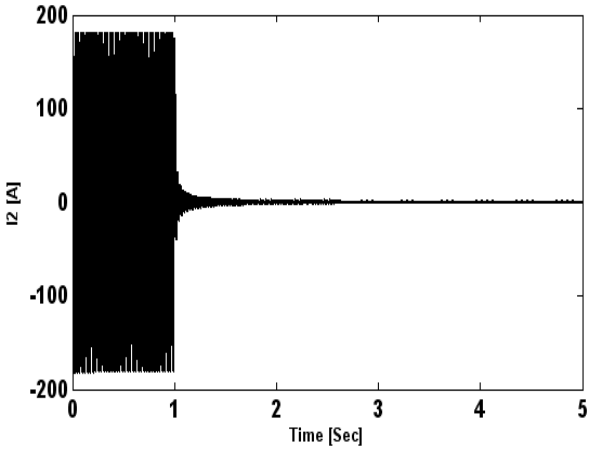

(b)

Fig.4. Time response of the LIM (a) Stator current, (b) rotor current

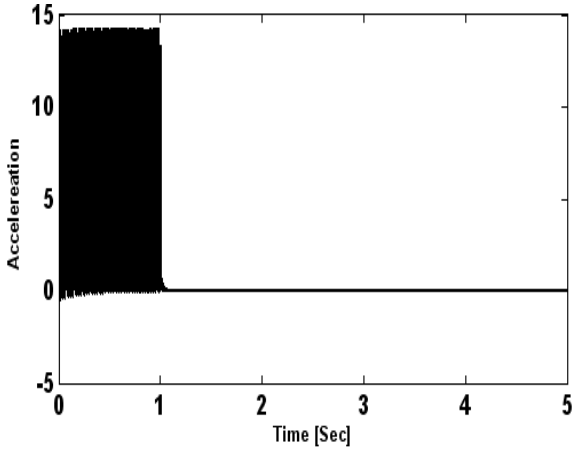

(a)

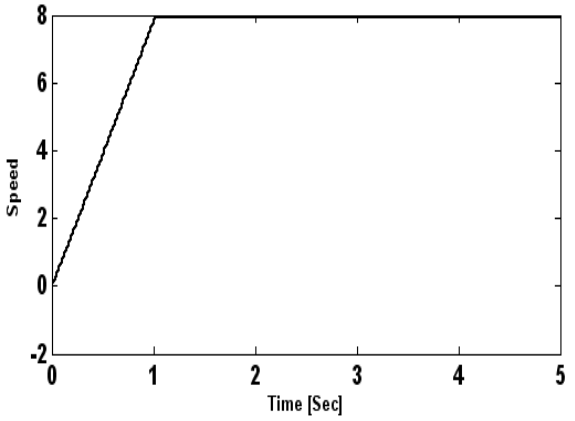

(b)

Fig.5. Time response of (a) Acceleration, (b) speed

4.1 The PID Controller

The PID controller is widely used as a feedback controller in industry. It calculates the error between an actual (measured) signal and a reference value and then minimizes this by adjusting the input of the system.

The PID controller is defined by the following equation:

$$u(t) = K_P e(t) + K_I \int e(t)dt + K_D \frac{d}{dt} e(t) \quad (20)$$

Where u(t) is the output of the PID Controller, K_p, K_I and K_d are the proportional, integrative and derivative gains, respectively and e(t) is the error signal which is defined as:

$$e(t)=r(t)-y(t) \quad (21)$$

Where r(t) is the reference value and y(t) is the output of the system[15].

The proportional term is the main gain. It changes the cuurent value of the error. A high proportional gain results in a large change in the output of the system for a certain error. In case of very high value of proportional gain, the system can be unstable. The integrative term is sum of the instantaneous errors over time which gives an accumulated offset to the output of the controller. The integral is then multiplied by the integrative gain and added to the controller output to decrease the rise time and eliminate the steady state error which cannot be accomplished by only with the proportional term. The last term of equation (20) facts on the sudden changes in the system such as any disturbance or noise which is not considered here. The block diagram of the PI controller and linear induction motor is shown in Figure 6.

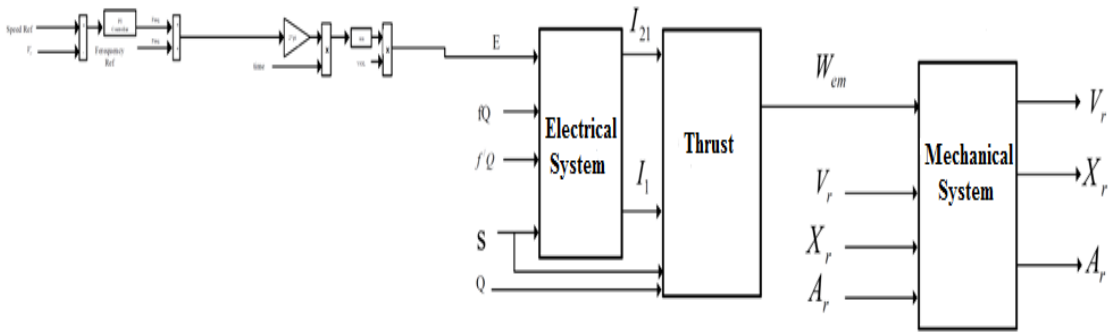

Fig.6. The block diagram of the system with PI controller

4.2 PI coefficients tuning by Particle swarm optimization

Particle swarm optimization (PSO) is a stochastic search method, which is proposed in 1995 [16-18]. The PSO algorithm maintains a swarm of individuals (called particles), where each particle represents a candidate solution. Particles follow a simple behavior: emulate the success of neighboring particles and its own achieved successes. The position of a particle is therefore influenced by the best particle in a neighborhood, P_{best}, as well as the best solution found by the particle itself, G_{best}. Particle position, x_i, are adjusted using:

$$x_i^{k+1}=x_i^k + v_i^{k+1} \quad (22)$$

where k represents the step size. The velocity is calculated by:

$$v_i^{k+1}= \omega v_i^k + c_1 r_1\{ P_{besti} - x_i^k \}+c_2 r_2 \{ G_{best} - x_i^k \} \quad (23)$$

Where ω is the inertia weight, c_1 and c_2 are the acceleration coefficients, r_1, r_2 ϵ U (0,1), P_{besti} is the personal best position of particle, and G_{best} is the best position of the particles. Note that r_1 and r_2 are random numbers.

V. SIMULATION RESULTS WITH PI CONTROLLER

In the following analysis, a disturbing force of 100% of the nominal load with a value of 1000 N is applied to the system at time 2s (see Figure 7). It is also seen in this figure that this opponent force reduces the rotor speed V_r from the reference value of 12m/s to 11.8m/s. Then the PI controller is activated before 3s, and leads the system to reach the reference rotor speed in an interval of 0.2s.

Figure 8, shows the response of the rotor speed with PI controller which is tuned by PSO. The results of this figure show that the disturbances and the frequency changes are reduced in this case which confirm the effectiveness of the PSO algorithm.

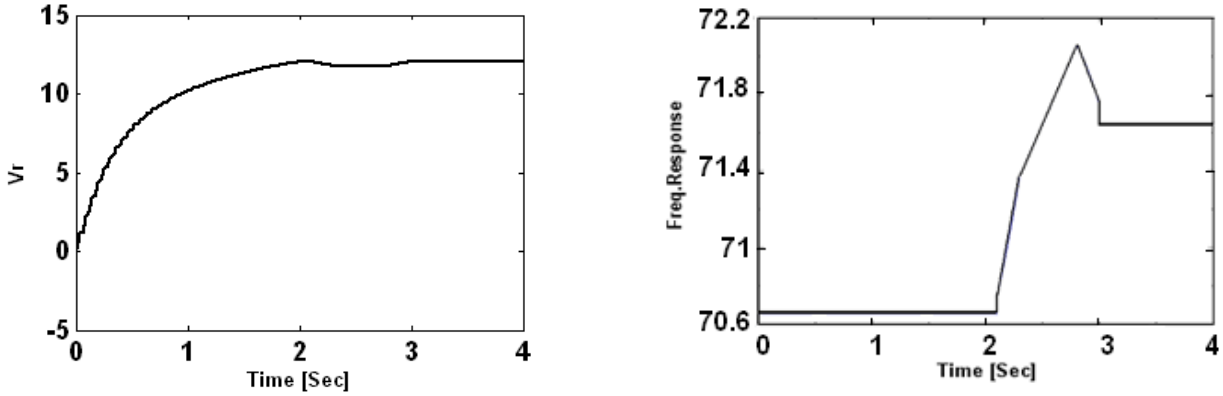

Fig.7. PI Controller response, manually tuned

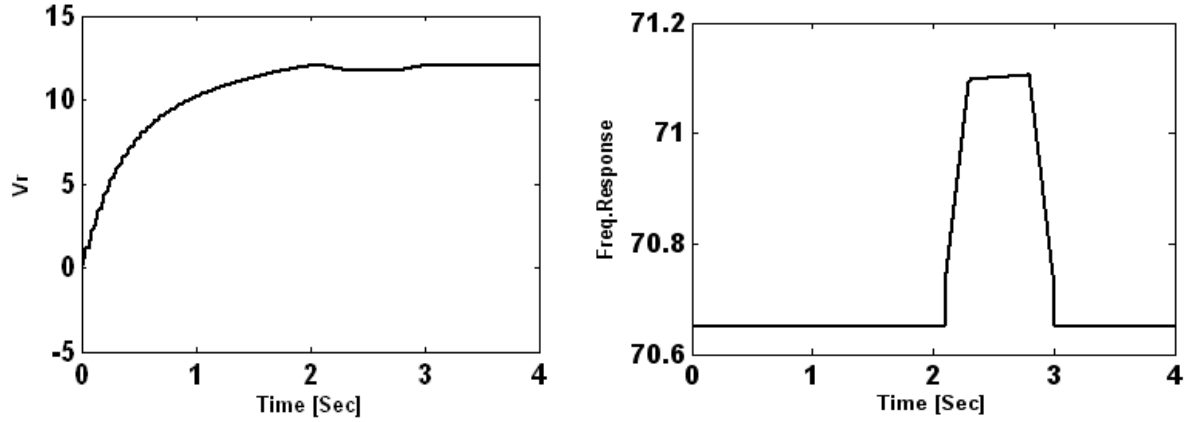

Fig.8. PI Controller response, tuned by PSO

VI. Conclusion

In this paper, the analysis of the dynamic response of the linear induction motor as an electromechanical system is done. A control strategy based on PSO technique is proposed to control the motor. To investigate the effectiveness of the proposed method, the dynamic model of the motor and the controller is simulated in MATLAB/Simulink environment. According to the obtained results, the PSO based PI controller has better accuracy and performance in comparison with the conventional PI controller.

Appendix A

Parameters and quantities for the LIM

Parameters	F (Hz)	V (Volt)	M (kg)	V_s (m/s)	τ(m)	D (m)	L_m (H)	L_2(H)	L_1(H)	R_2 (ohms)	R_1 (ohms)
LIM	60	9.36	300	10.4	0.0867	0.574	-0.064	0.0012	0.0029	0.332	0.641

References

[1] Chapman, S. Electric Machinery Fundamentals. New York: McGraw-Hill.

[2] M. Comanescu, L. Xu, "An improved flux observer based on PLL frequency estimator for sensorless vector control of induction motors," *IEEE Transactions on Industry Electronics,* vol. 53, pp. 50- 56, 2006.

[3] Yuichiro Nozaki, Terufumi Yamaguchi and Takafumi Koseki, "Equivalent Circuit Model of Linear Induction Motor with Parameters Depending on Secondary Speed for Urban Transportion System," *Department of Electrical Engineering,* 113-8656.

[4] J. Duncan, "Linear Induction motor-equivalent circuit model," *IEE Pro ceedingsof Electric Power Applications B,* vol. 130, pp. 51-57, 1983.

[5] A.S. Gercek, V.M. Karsli, "Performance prediction of the single-sided linear induction motors for transportation considers longitudinal end effect by using analytical method," *Contemporary Engineering science,* vol. 2, pp. 95-104, 2009.

[6] W. Xu, J.G. Zhu, Y. Zhang, Z. Li, Y. Li, Y.Wang, Y. Guo,W. Li, "Equivalent circuits for single-sided linear induction motors," *IEEE Transactions on Industry Applications,* vol. 46, pp. 2410 2423, 2010.

[7] Abbas Shiri, Mohammad Reza Alizadeh Pahlavani, Abbas Shoulaie, "Secondary Back-Iron Saturation Eects on Thrust and Normal Force of Single-Sided Linear Induction Motor," volume 2012, Article ID acte00111, 9 Pages, 2012.

[8] E.R. Laithwaite and S.A. Nasar, "Linear-Motion Electrical Machines," *Proceedings of the IEEE*, vol. 58, no.4, April 1970.

[9] Ali Suat Gerçek, Vedat M. Karsl, "Performance Prediction of the Single-Sided Linear Induction Motors for Transportation Considers Longitudinal End Effect by Using Analytic Method," *Contemporary Engineering Sciences*, vol. 2, no. 2, 95-104, 2009.

[10] David C. Meeker, Michael J. Newman, "Indirect Vector Control of a Redundant Linear Induction Motor for Aircraft Launch," July 3, 2008.

[11] Amir Zare Bazghaleh, Mohammad Reza Naghashan and Mohammad Reza Meshkatoddini, "Optimum Design of Single-Sided Linear Induction Motors for Improved Motor Performance," *IEEE Transactions on Magnetics*, vol. 46, no. 11, November 2010.

[12] Boucheta, A, "Adaptive backstepping controller for linear induction motor position control," *Acompel : The International Journal for Computation and Mathematics in Electrical and Electronic Engineering,* vol. 29, no. 3, pp. 789-810, 2010.

[13] A. Boucheta, I. K. Bousserhane, A. Hazzab, P. Sicard, and M. K. Fellah, "Speed Control of Linear Induction Motor using Sliding Mode Controller Considering the End Effects," *Journal of Electrical Engineering & Technology,* vol. 7, no. 1, pp. 34-45, 2012.

[14] Mohammad Reza Satvati, Sadegh Vaez-Zadeh, " End-Effect Compensation in Linear Induction Motor Drives," *Journal of Power Electronics*, vol. 11, no. 5, September 2011.

[15] Ang, K.H, "PID control system analysis, design, and technology," IEEE Transactions on Control Systems Technology 13(4): pp. 559-576, 2005.

[16] Rabab M. Ramadan and Rehab F. Abdel-Kader, "Face Recognition Using Particle Swarm Optimization-Based Selected Features," *International Journal of Signal Processing, Image Processing and Pattern Recognition,* vol. 2, no. 2, June 2009.

[17] Peter J. Angeline, "Using selection to improve particle swarm optimization," *In Proceedings of the 1998 IEEE Congress on Evolutionary Computation*, pages 84-89, Piscataway, NJ, USA, 1998.

[18] Yuhui Shi and Russell Eberhart, "A modified particle swarm optimizer," *In Proceedings of the IEEE International Conference on Evolutionary Computation*, pages 69-73, 1998.